Maturing EMCCD Photon-Counting with Variable Multiplication Gain Imaging for a Coronagraphic Instrument

Udayan Mallik[a,*], **Peter Petrone**[b], **Dominic J. Benford**[a]

[a]National Aeronautics and Space Administration, Goddard Space Flight Center, Greenbelt, Maryland, 20771, United States of America

[b]Sigma Space Corporation, Lanham-Seabrook, Maryland, 20706, United States of America

Abstract. This is an introduction to a US Government Program that conducted high-contrast imaging experiments with an Electron Multiplying Charge Coupled Device (EMCCD) in an interferometric coronagraph. This report will introduce the concepts of "Charge Blooming" and "Starlight Saturation" in the context of high-contrast astronomical imaging. These phenomena adversely affect the performance of high-contrast photon-counting instruments that do not use a mask to physically block starlight in the science channel of the coronagraph. The problems will be presented with the help of images taken with a commercial EMCCD camera in the Visible Nulling Coronagraph at the Goddard Space Flight Center (GSFC). A new clocking scheme for EMCCDs – Variable Multiplication Gain Clocking – will be proposed as a means for suppressing horizontal blooming and starlight saturation in an astronomical camera. This opening report from the program will conclude with an introduction to a new controller for high-contrast imaging with EMCCDs in coronagraphs. This controller is being designed to allow a single frame from an EMCCD to be scanned in multiple modes – photon-counting and digitization – to enable direct imaging of an exo-planet and wavefront control of a coronagraph, simultaneously.

Keywords: Electron Multiplying Charge Coupled Device, High-Contrast Imaging, Photon-Counting Imaging, Coronagraphic Instrument, Visible Nulling Coronagraph, Exoplanet.

*Corresponding Author, E-mail: u.mallik@hotmail.com

1 Introduction

The National Aeronautics and Space Administration (NASA) was directed by the Decadal Survey for Astrophysics and Astronomy, New Worlds and New Horizons[1], 2010, to develop technologies for a space-borne, high-contrast imaging and spectroscopy mission as its top-ranked medium term space project. NASA, as a result, funds a number of investigations that demonstrate space technologies for new missions, especially missions that will answer critical questions regarding the beginning, the evolution and the future of the universe, and that of the objects within it such as galaxies, stars and planets. The Visible Nulling Coronagraph (VNC) at the GSFC has received four grants from the Technology Demonstration for Exoplanet Mission (TDEM) project office (at NASA Headquarters),[2,3,4,5] to investigate an interferometric type coronagraph architecture that can be used to directly image an exoplanet around a nearby star. An Internal Research And Development (IRAD) program, was created at the GSFC to complement these grants, and initiate an investigation of high-contrast imaging with an EMCCD in a coronagraphic instrument. This program found that a number of technical problems present themselves when an EMCCD is used in the science channel of a coronagraph. Construction of a new controller for a Teledyne e2v EMCCD, was therefore initiated at GSFC to overcome these problems. This controller is also expected to help other coronagraphic instruments that have been funded by the TDEM office.[6,7,8]

Herein is a report from the group at GSFC that conducted imaging experiments with an EMCCD in a high-contrast instrument. A large number of efforts in technology maturation will be presented in this report. These efforts, it is expected, will culminate in a high-contrast instrument imaging an exoplanet around a star with an EMCCD from space. The first two sections, and the three sub-sections within them, will set a backdrop for the high-contrast experiments that will be presented later in the document. This is with the aim that this report be complete and provide full justification for the program. A preliminary report from this program was published as a conference proceedings at SPIE, San Diego in 2015.[9] This report paints the full picture for this program – complete with an elaborate background, an in-depth literature review, additional sections that justify a new controller for EMCCDs and a discussion of simulated images to demonstrate the expected operation of this new controller.

This report from here on in is formatted as follows. Section 2 will provide a comprehensive background to this program. Section 2.1, will describe the architecture of an EMCCD and discuss the difficulties of using this device in a CoronaGraphic Instrument (CGI). Section 2.2, will discuss the current state of the art in photon-counting imaging on an astronomical space telescope. Section 2.3, will briefly discuss the visible nulling coronagraph instrument, at the GSFC. In Sec. 3, saturation and charge blooming in an EMCCD will be introduced in the context of high-contrast imaging. This will be done with the help of high-contrast images taken with a commercial EMCCD camera in an interferometer. In Sec. 4, new imaging techniques will be introduced that can help an EMCCD suppress starlight saturation and horizontal blooming, to operate more effectively in a coronagraph. Section 5, will present a case for designing a new controller for an EMCCD in a CGI. This report will conclude with a summary and a discussion of future work in Sec. 6.

2 Background

Photon-Counting EMCCDs have been with us for more than a decade.[10] High-contrast imaging instruments – for directly imaging an exoplanet, around a nearby star,

have been in development for a similar period of time. A high-contrast imaging experiment in a laboratory neither uses an experimental setup nor an experimental method to image an exoplanet around a nearby star. A laboratory experiment in high-contrast imaging is geared towards demonstrating a simple number – the "contrast ratio" – a number generated by dividing the amount of light from a star after starlight suppression and nulling by the amount of light from the star before starlight suppression and nulling. High-contrast imaging instruments therefore use statistical methods to produce such a contrast-ratio. As a result nearly all research groups in this field use CCD or CMOS imaging cameras to report their science.

Imaging an exoplanet is however distinct from high-contrast imaging. Imaging an exoplanet is a physics-based problem. A single photon reflected by an exoplanet generates a photo-electron in an imaging array. The signal from that photo-electron is reported to a processor with the help of sensitive readout circuits. This part of the problem is not considered in a high-contrast experiment. Space missions that will image exo-planets expect to rely on an EMCCD to both suppress starlight and image an exoplanet in a CGI. An EMCCD matures a space based CGI out of the realm of high-contrast instruments and into the realm of exoplanet imaging instruments. The first sub-section addresses this topic.

The second sub-section (Section 2.2) provides an introduction to photon-counting sensors, complexities of space based photon-counting and photon-counting with an EMCCD in space. An EMCCD was designed to image a low-light scene by amplifying the integrated image signal in its charge multiplication register. Maturing low-light imaging capability with the ability to detect single-photon events in a large format CCD type array makes the EMCCD a very interesting detector in space astrophysics. The ability to count photons allows an EMCCD to compete with a Microwave Kinetic Inductance Detector (MKID)[11] and a Transition Edge Sensor (TES)[12] (both cited as energy resolving detectors[13]), for a spot on a space based telescope as a large-format single-photon-counting detector array. An EMCCD offers the additional advantage of being a dense integrating type array that can be scanned in analog mode for high-contrast imaging. Hence the section's title – Maturing Multiplying Type CCDs with Photon-Counting Technology for Space Astronomy.

An improvised lyot coronagraph provides space astronomy with a means to directly image exoplanets on the Hubble Space Telescope (HST).[14] This will mature with sophisticated four-quadrant phase-mask coronagraphs, lyot type coronagraphs and aperture masking interferometry on the James Webb Space Telescope (JWST).[15,16,17] All these are passive starlight suppression topologies that rely on static structures to suppress starlight and create a dark region around a star where exoplanets can be imaged. A new generation of coronagraphs that use active elements like Micro-Electro-Mechanical System (MEMS) deformable mirrors and Spatial Filter Arrays (SFA)[18] and passive elements like masks to suppress star-light are in development. A visible nulling coronagraph is one such coronagraphic topology. The final sub-section (Section 2.3) describes this instrument. The VNC is an active wavefront control system that suppresses starlight by using destructive interference of waves. It does not use a physical blocking mask – like other coronagraphic topologies – to suppress stellar light. A VNC conserves all light, no light is discarded. One arm of the interferometer implements starlight suppression and wavefront control while the other arm implements nulling and exoplanet imaging operations. The last sub-section describes how a VNC will mature space astronomy with an instrument that can view very dim objects around nearby stars and do so around the very dimmest stars in space.

The purpose of this section is to introduce the basic principles of imaging with an EMCCD, the complexities of high-contrast imaging with an EMCCD, photon-counting imaging in space for coronagraphy and the basic physics of interferometric coronagraphy. It sets up the complexity of each element in isolation and of combining the individual elements in the most stressing configuration for each element – briefly introducing the drivers for the program that is presented in this report.

2.1 Maturing Coronagraphic Instruments with Electron Multiplying Charge Coupled Devices

The EMCCD has been derived from a CCD by adding an electron multiplying cascade stage to the basic CCD architecture. This new stage is used to amplify the integrated image and enhance the performance of a CCD in a low-light environment. In a regular CCD, light will generate photo-electrons that are proportional in number to the intensity of the beam incident on the focal plane. The charge thus generated represents an image. This charge, at the end of image formation is vertically shifted to a read-out row register at the bottom of the focal plane on a row-by-row basis. The charge is then horizontally shifted out of the chip through a read-out amplifier.

A frame-transfer type EMCCD is comprised of a regular CCD imaging area, a bank of storage registers (pixels in the storage area of the sensor) and a hybrid read-out register (Figure 1). The read-out operation of this type of a CCD is much more complex. In an EMCCD, integrated charge is first vertically shifted from the imaging area to a storage area. The chip contains as many storage elements in the storage area as it contains pixels in the imaging area. The shifting of charge from the imaging to the storage area is called the "frame transfer phase" of read out. Frame transfer is implemented in the sensor because

it takes very little time and acts like a global electronic shutter. It prevents introduction of motion induced smearing artifacts when the image is amplified and read-out of the chip. Mechanical shuttering is recommended during frame transfer to prevent image integration and smearing during the "frame transfer" process itself. An EMCCD amplifies the very minutest signals (as low as those from single photon events). Smearing is a major concern in a camera system with an EMCCD detector. Frame transfer and mechanical shuttering are means for preventing pronounced smearing artifacts in a multiplying type CCD. The "line transfer phase", transfers charge on a row-by-row basis from the storage area to the read-out (row) register at the bottom of the chip. The read-out register of an EMCCD has two operating modes. The first is a standard CCD read-out mode. In this mode read-out row register (see "1056 Register Elements" in Fig. 1) operates like a regular CCD read-out row register, and horizontally shifts integrated charge out of the chip through an amplifier. The second read-out mode is called the Charge Multiplication Read-out Mode. Charge multiplication is implemented by shifting integrated charge through the multiplication registers (see "604 Multiplication Elements" at the bottom of Fig. 1), and not the regular CCD register, by reversing the sequence of the read-out clocks. The multiplication elements use a phenomenon called "Impact Ionization"[19] to amplify integrated the image signal. Impact ionization works by adding an amount of charge to a multiplication element that is proportional to the charge already present in it. Impact ionization is brought about by using

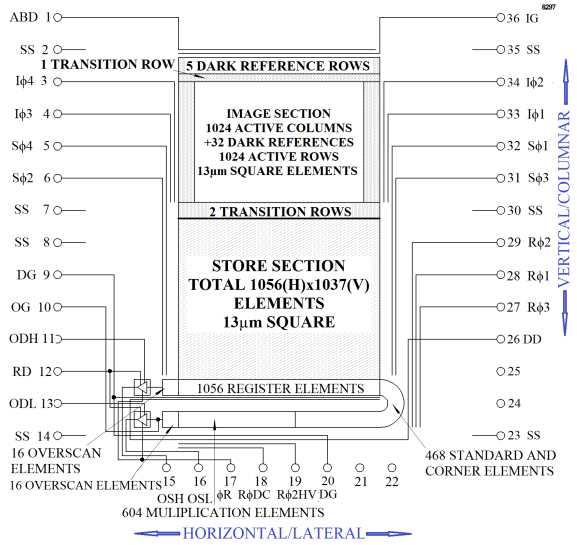

Fig 1 Architecture of a CCD201 chip. Horizontal/Lateral and Vertical/Columnar movement of charge will be discussed throughout this report. These two directions are therefore prominently marked in this figure for future reference. Image re-produced with permission from Teledyne e2v.

an additional high-voltage multiplication gain clock in the readout sequence. Its amplitude usually varies between 20 and 50V – where 50V produces the maximum gain. The multiplication row register uses a separate amplifier to read-out the amplified signal to a processor. Multiplication gain imaging allows a CCD to implement single-photon-counting imaging in a large format array.

In a Teledyne e2v CCD201 EMCCD, it has been shown that single-photon-counting imaging can be implemented with a 91% probability of single-photon event detection [20] (for a part of the visible wavelength, usually around 550nm). Single-photon-counting imaging refers to the incidence of a single photon on a pixel inside a photo-detector array and its reading out to a processor by a readout circuit. The probability of detection is mainly limited by the quantum efficiency of the CCD201 detector (96%).[21] In other words sensing and read-out – especially the avalanche stage of an EMCCD – are decoupled. When a higher or lower energy photon is incident on the detector (where the QE is lower), the signal from this photon, if detected by the sensor, will be successfully read out without much signal corruption by the readout circuits. This has important ramifications in UV astronomy that will be discussed in Sec. 2.2. Detector technology however keeps getting better: Developments in coatings technology for EMCCDs have demonstrated near 100% QE (in some visible wavelengths) in laboratory settings. Photon-counting experiments with these detectors have not yet been reported.[22] However, when such experiments are reported, they will increase the probability of detecting a single photon above the present 91%.

A planet finder mission (like EPIC or Exo-S) is expected to use an internal or external coronagraph to image exoplanets around nearby stars. An EMCCD is expected to be the pre-eminent detector technology for such an instrument.[23,24,25] Exoplanets are expected to be very dim astronomical objects as seen by astronomical telescopes ($<<$ 1 photon/sec for the WFIRST coronagraph)[26] (also see Fig. 2 for a distribution of planet-photon counts expected per square meter of telescope area for 5 classes of stars). Integrated planet light is $10^{10} - 10^{11}$ times dimmer than the integrated starlight. 'Integrated' refers to all the light collected by the aperture for a planet and star system. This light is then distributed into a point spread function (PSF) in the focal plane, such that the spatial integral of the PSF of the planet is $10^{10} - 10^{11}$ times dimmer than the spatial integral of the PSF of the star. However, the star – even after starlight suppression – is much brighter than the exoplanet. A coronagraphic instrument is therefore expected to produce a high-contrast image – where a bright star and a dim planet will be imaged together on the same focal plane in very close proximity of each other.

Photon-counting imaging is expected to be required

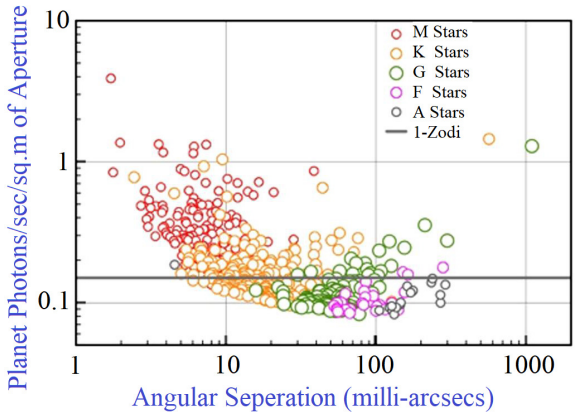

Fig 2 A plot that shows the # of photons collected from an exoplanet per square meter of telescope area vs. angular separation. A very few planet photons are collected from the exoplanet.

from any camera that will image exoplanets in the science channel of a space based coronaraph.[27,28] This instrument – for the sake of simplicity – will also prefer to use a single detector for both UV and visible wavelengths. An EMCCD affords both these options to a CGI. An EMCCD must operate in a very high-gain mode to implement photon-counting imaging. A multiplying type CCD in a high-contrast imaging instrument will therefore suffer from two technical problems – "Charge Blooming" and "Starlight Saturation". These problems especially affect any type of coronagraph that maintains both a star and its planetary system in the imaging field.

Charge blooming causes an enlargement of the star on the focal plane. The closest region in space around the star where a coronagraph can create a dark hole (to image light reflected by a planet) – The Inner Working Angle (IWA) – is extended out by many λ/d. This can have a drastic effect on a coronagraph's ability to image inner planets, especially rocky terrestrial planets and other nearin planets that are expected to be found very close to the star. This phenomenon affects non-masking type coronagraphs more than masking type coronagraphs. However, a masking-type coronagraph will see the same effect in the event of a telescope jitter or a telescope mis-pointing.

Starlight saturation adversely effects high-contrast imaging algorithms in a coronagraph. Algorithms attempt to maintain the central stellar peak at or below 84% of full well. This is because the PSF is normalized such that its integral is unity. Its central core, to a radius of $\theta = 1.22\lambda/D$ contains 84% of the energy, and a detector pixel is therefore sized to account for that 84% of the energy.[29] However, it is very difficult to maintain this criterion in a photon-counting EMCCD, because starlight saturates in a high-gain detector. In conjunction with charge blooming, starlight saturation makes operation of a CGI very difficult, making imaging an exoplanet with an EMCCD a very difficult task.

2.2 Maturing a Multiplying CCD with Photon-Counting Technology for Space Astronomy

The Origins[30] road-map defines detectors as "the single most important technology that determines the ultimate performance of our observatories." It further goes on to note that for the whole range of future Origins missions, for imaging and spectroscopic observations, achievements in advanced focal-plane technologies will be critical, if we are to fully benefit from the inherent sensitivities being designed into future astronomical mission-concepts.

Davinci,[31] TPF-C,[32] TPF-I,[33] EPIC,[34] LUVOIR,[35] Exo-C,[36] Exo-S[37] and WFIRST[38] are all examples of high sensitivity mission concepts that aim to detect life around a nearby star on an exoplanet. They call for a UV-VIS (and in some cases NIR) photon-counting camera to conduct their science. NASA is investigating a large number of technologies to implement large-format photon counting imaging.[39,40] UV Galaxy Survey missions are also driving the search for large format photon counting detectors. Some of these cameras use superconducting sensors[39] that make a spacecraft cumbersome (because they need a coolant) and/or noisy (because of vibrations from the cooling mechanism).[24] A large and heavy storage tank for coolants, to cool a detector on a space telescope,[41,42] limits the size and lifetime of a flagship class mission. This makes it hard to justify the cost of very large aperture systems in space to conduct meaningful exoplanet science. Vibrations on the other hand, limit the effectiveness of wavefront control systems inside a CGI. Exoplanet science therefore seeks photon-counting detectors that can operate at moderate temperatures, which can be achieved with Thermo-Electric Coolers (TEC) or with passive cooling methods.

An EMCCD operates at moderate temperatures (163K) and with reasonably low voltages (15V – 50V). An (Teledyne e2v) EMCCD, in addition, can be operated with low effective read noise ($\leq$0.1e$^-$) at reasonably high-speeds (20MHz).[10,43] This type of detector, is therefore highly desirable for low-light imaging applications – especially single-photon-counting applications – on long duration missions in space. A Teledyne e2v Technologies CCD201 is therefore the baselined detector for both science focal planes in the WFIRST coronagraph – the imager and the integral field spectrometer.[38,44]

In the UV wavelengths, Micro-Channel Plates (MCPs) and other photon-counting detectors that have flight heritage in the UV wavelengths on NASA missions – for example the Hubble UV sensor – use very low QE detectors. These detectors have QE in the 10% - 25% range.[45] A

low QE detector in the science camera of a telescope increases the amount of time a telescope spends on each target. This reduces the amount of science returned by space missions in astrophysics. Imaging in the UV-VIS wavelengths with a Solid State Detector (SSD) is one of the ways US scientists are attempting to increase the Quantum Efficiency (QE) of large format photon-counting UV-VIS cameras.[22] An EMCCD is such an SSD technology. A Teledyne e2v EMCCD with a delta doped imaging surface offers an opportunity to increase the QE of UV imaging cameras to 50%.[46]

An EMCCD is a very complex device and a substantial amount of work has gone into developing it as a detector that can image exoplanets in photon-counting mode from space. Here are some highlights. The EMCCD at Teledyne e2v was primarily designed to create a high-yield detector for ground based applications in the commercial market. As a result, a number of optimizations were incorporated into the device that degrade its performance over time,[47] and, in high-radiation environments.[24,38] However, many applications in space physics view an EMCCD as an ideal detector for low-light imaging instruments.[25,48] The WFIRST CGI is one such instrument. An EMCCD is therefore being characterized for space flight at the Jet Propulsion Laboratory (JPL).[38] A commercial controller has been earmarked for this task[49]. It is expected that this commercial device will be converted to a controller for space. A number of techniques have been proposed by Teledyne e2v for imaging low-light scenes with an EMCCD.[50] A group at NüVü Caméras has published multiple proceedings papers to describe their work with EMCCD sensors in the fields of characterization,[51] long exposure astronomy,[52] and photon-counting imaging.[43,53] Other groups have also published papers that discuss techniques for counting photons with an EMCCD.[10,54] In addition, since an EMCCD amplifies both signal and noise in its multiplication register, a substantial effort has been made to understand its noise function.[55,56] This knowledge is critical when predicting a camera's performance on long duration, very low-light/photon-counting missions in space. On the controller front, multiple groups have reported controller architectures for an EMCCD.[9,48,49,57] The group from NüVü Caméras has reported the best results in photon-counting imaging with an EMCCD with their CCD Controller for Counting Photons (CCCP).[49] However, only the GSFC group has reported substantial high-contrast experiments with an EMCCD in a coronagraphic instrument (with a commercial controller).[9] A PhD dissertation at the University of Sheffield reported similar observations, with respect to charge blooming, when an EMCCD was used in spectroscopic experiments in stellar astronomy.[58]

An EMCCD is a powerful tool for study in space astronomy. High-contrast photon-counting with an EMCCD is a new and unknown frontier in space instrumentation. This is one of the first reports to describe the result when a high contrast instrument is coupled to a photon-counting EMCCD.

2.3 Maturing Space Astronomy with a Visible Nulling Coronagraph Instrument

The GSFC Visible Nulling Coronagraph (VNC)[18,59] is one of the candidate technologies for imaging exoplanets around nearby stars. This type of an architecture for coronagraphs, is being investigated by a number of groups[60,61,62,63,64,65,66] to directly image exoplanets on future space missions. A VNC is one of the known internal coronagraph topologies that can theoretically operate with all types of telescope apertures – Filled, Sparse, Diluted and Segmented. It is expected that a space interferometer will open a new chapter in space astronomy and allow the dim details surrounding nearby stars to be imaged with a space based telescope. The VNC will therefore be briefly described in this section as the final host of a planet finder camera at GSFC.

The GSFC VNC[2] is a modified Mach-Zehnder type interferometer. It splits and then recombines starlight to create two arms of an interferometer (Figure 3). The VNC is also an image feedback based active control system. A Deformable Mirror (MMA) is used in one arm of the interferometer to suppress starlight by imparting specific phase-shifts within specific regions of an incoming telescopes beam. On-axis starlight is imparted a 180^o phase-shift and nulled (because of destructive interference). The off-axis planet light receives additional phase-shifts, and therefore, continues to remain visible in the science channel of the interferometer. The two arms of the interferometer are channeled to two camera systems – a

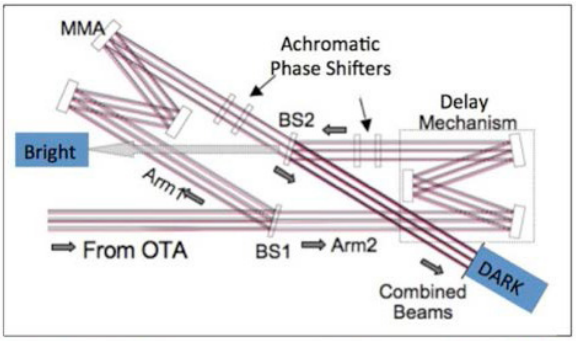

Fig 3 An optical schematic for the VNC. A VNC is a modified Mach Zehnder Interferometer. The deformable mirror and delay line mechanisms impart phase-shifts to the beam and implement starlight suppression and nulling. Achromatic Phase Shifters allow the instrument to operate with a broadband beam.

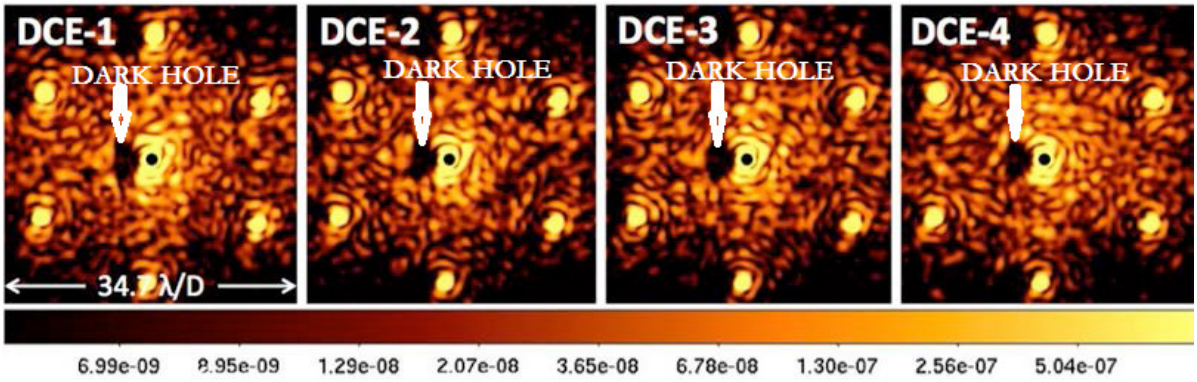

Fig 4 Images from VNC's Data Collection Event (DCE) for the Strategic Astrophysics Technology, Technology Demonstration for Exoplanet Mission (SAT, TDEM) 2012, final report. The four images were created after post processing images from a CMOS "DARK channel" camera in the VNC. The 512×512 images are the average of the last 3,800 frames showing the science focal plane on a log-scale. The central leakage is 10^4 darker than without any nulling and the region labeled "dark hole" is 10^5 times darker yielding an overall contrast of 5.5×10^{-9} when averaged over the dark-hole region. The dark-hole region extends from $1 - 4\lambda/D$ and in a 60 degree arc left of center. Image plate scale is 16.8 pixels per λ/D and the images shows a full FOV of $30.5 \times 30.5\lambda/D$. The experiment to find the VNC's null capability was repeated 4 times over four days to prove that the instrument and its wave-front control algorithm can robustly and repeatedly reach the same null depth in an area around the central star. The planet light – when present – will appear in that dark region next to the central peak.

wave-front control camera ("BRIGHT" in Fig. 3 (a Complimentary Metal Oxide Semiconductor (CMOS) camera)) system and a science camera system ("DARK" in (Photon-Counting EMCCD Camera)).[18,59] An interferometric type coronagraph does not block starlight in the science channel of the instrument. Starlight is used to, either implement coarse wavefront control algorithms in the "BRIGHT" channel or to implement fine wavefront control and nulling in the "DARK" channel. However due to limitations in MMA technology, starlight is never fully suppressed. Some starlight continues to be visible in the science channel (DARK) even after starlight suppression and nulling (Figure 4).

The instrument's wave-front control and nulling algorithm is designed to maintain starlight at or below 84% of full-well. This is done both physically with filters and electronically by adjusting the integration time of the sensor. The intensity of the star in the central lobe, and six side lobes (Figure 4), must be accurately measured to compute a contrast ratio for the instrument. The VNC has reported a contrast milestone of 5.5×10^{-9} contrast ratio in 2012 with a 1% narrow-band beam.[2,59] An EMCCD camera was initially used as the science detector in this experiment. However, the VNC failed to operate with the saturated, and horizontally and vertically bloomed images. The EMCCD camera was therefore abandoned. A CMOS camera was used its instead to reach the milestone.

An interferometric type coronagraph does not use a mask to suppress starlight in the science channel of the instrument. Starlight is used to, implement wavefront control or nulling algorithms. A considerable amount of starlight continues to be visible in the science channel of a VNC after starlight suppression. On a large space-based telescope – such as the Large UV/Optical/InfraRed surveyor (LUVOIR) – an internal coronagraph can saturate a detector on bright stellar sources. The next two sections present problems that are encountered when an EMCCD is used in the science channel of an interferometric coronagraph and the solutions that have been proposed to solve them.

3 Imaging Experiments with an EMCCD in a High-Contrast Instrument

A small Michelson Interferometer experiment has been set up to test all candidate technologies for the VNC in a interferometer before they are inserted in the instrument. This test-bed is called the Null Control Breadboard (NCB). The output beam from the interferometer was designed to mimic the beam pattern of the science channel in the VNC. This was achieved by inserting a 169 segment "Lyot Mask" in the optical path of the combined beam. A number of mirrors relay the beam to an EMCCD camera that is used to demonstrate the performance of EMCCD technology in a coronagraph. A Barlow lens is placed just before the camera to magnify the image and create adequate spatial sampling on the detector.

It is well known that a very bright object has a tendency to bloom on a CCD and EMCCD. "Vertical (columnar) Charge Blooming" occurs when a very bright object is imaged with a CCD type detector. A bright object saturates by creating more electrons than can be stored in the integration well of a CCD pixel. The excess charge created by a bright source spills over into neighbouring pixels in

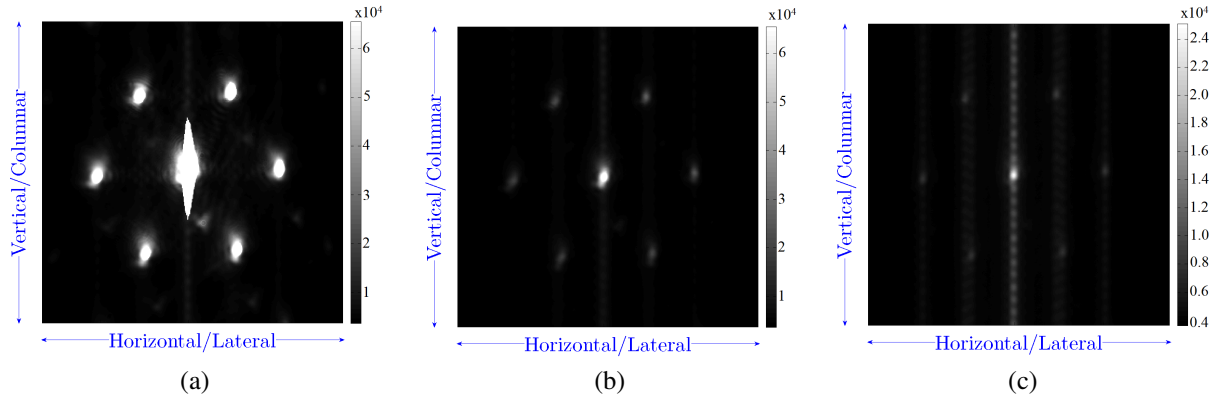

Fig 5 Blooming in the science channel of a nulling type interferometer. The gain is set to a negligible value (approx. 1). (a) An image with a 10ms integration time. (b) An image with a 1ms integration time. (c) An image with a 0.1ms integration time. The central star in (a) is blooming and saturated. As integration time is reduced, a marked loss in signal-to-noise ratio is observed. The vertical streaking is caused by the absence of a mechanical shutter. When a mechanical shutter is introduced the streaking is restricted to half the image (top or bottom half). The top or bottom half is selected by a software switch. The purpose of this switch is unclear and the matter is under investigation.

the vertical (columnar) direction. Potential barriers prevent blooming into adjacent pixels (i.e. in the horizontal (lateral) direction). Such barriers do not exist in the vertical (columnar) direction.[67] There exist electronic means to suppress charge blooming. However, these methods are known to suppress a detector's QE.[68,69,70] Figure 5 shows the setting-in of vertical (columnar) blooming in an EMCCD. Since the blooming artifact is not a feature of the object being imaged, it is in effect a distortion of the speckle pattern of the star-planet system. As a detector artifact, this distortion cannot be corrected by wavefront control algorithms. A proper Airy pattern is central to a coronagraph's operation. Vertical blooming corrupts the Airy pattern and thus the operation of the coronagraph. In an image based active wave-front control system, like the VNC, this is a debilitating problem.

In a CGI, a high-gain EMCCD saturates the signal from a bright star when it amplifies the image with uniform gain (Figure 6). This is the second problem – "Saturation". The NCB source, while weaker than the source in the VNC, is still a very bright signal. In the next experiment, a neutral density filter was introduced after the laser to reduce the amount of flux entering the interferometer. The integration time was set to 1.7ms. Five images were collected with the camera's gain set to (a) No Gain (Figure 6a), (b) (approx) 1.5 (Figure 6b), (c) (approx) 5 (Figure 6c), (d) (approx) 10 (Figure 6d), (e) Max Gain (approx) 1000 (Figure 6e), respectively. The starlight saturates in Fig. 6c when the gain is still $0.15\% \times$Max Gain . At Max Gain, speckles become highly visible (Figure 6e), but the area around the central star and the six side-lobes also begins to saturate. The star and the side-lobes also build up a "horizontal blooming" artifact. This artifact is caused by surface trapping – an effect seen when high-gain is applied to pixels that contain a large amount of signal.[71] As the size of the large integrated charge packet increases with multiplication, it comes into contact with surface traps that capture the signal and release a part of it into the following pixel (hence it is only in one direction). Surface trapping leads to reduced Charge Transfer Efficiency (CTE) and the reduced CTE creates a bright streak in an image that follows bright pixels. This damages the performance of a high-contrast instrument in two ways – it distorts the speckle pattern of the star, and makes it impossible to image an exoplanet very near the bright object. Unless corrected, high signal CTE may limit the effective dynamic range of some measurements.

Horizontal blooming is now framed in the context of astronomical imaging. An 8m telescope can collect 10^{11} photons/sec (numbers between 8m and 16m have been cited as an aperture size for LUVOIR). Figure 4 shows that central peak after starlight suppression and nulling is allowed to remain at a 10^{-7} - 10^{-6} contrast state compared to the "DARK HOLE" which on average is at a 10^{-9} contrast state. This would imply that the area of the focal plane that is not nulled continues to receive 10^4 - 10^5 photons/sec. Assuming 1s integration time, if every photon generates a single photo-electron, at gain 5000, the star would be amplified to 10^4*5000 or 10^5*5000 e^-. The maximum capacity of the multiplication register is 800k e^- – much lower than the roughly millions of e^- being generated by the star. This will produce a large horizontal blooming artifact in the image and have the effect of cutting in half the number of pixels that can detect exoplanets (because horizontal blooming is unidirectional).

This section introduced us to the complexities of high-contrast imaging with a high-gain EMCCD. The imaging architecture of an EMCCD introduces artifacts in an

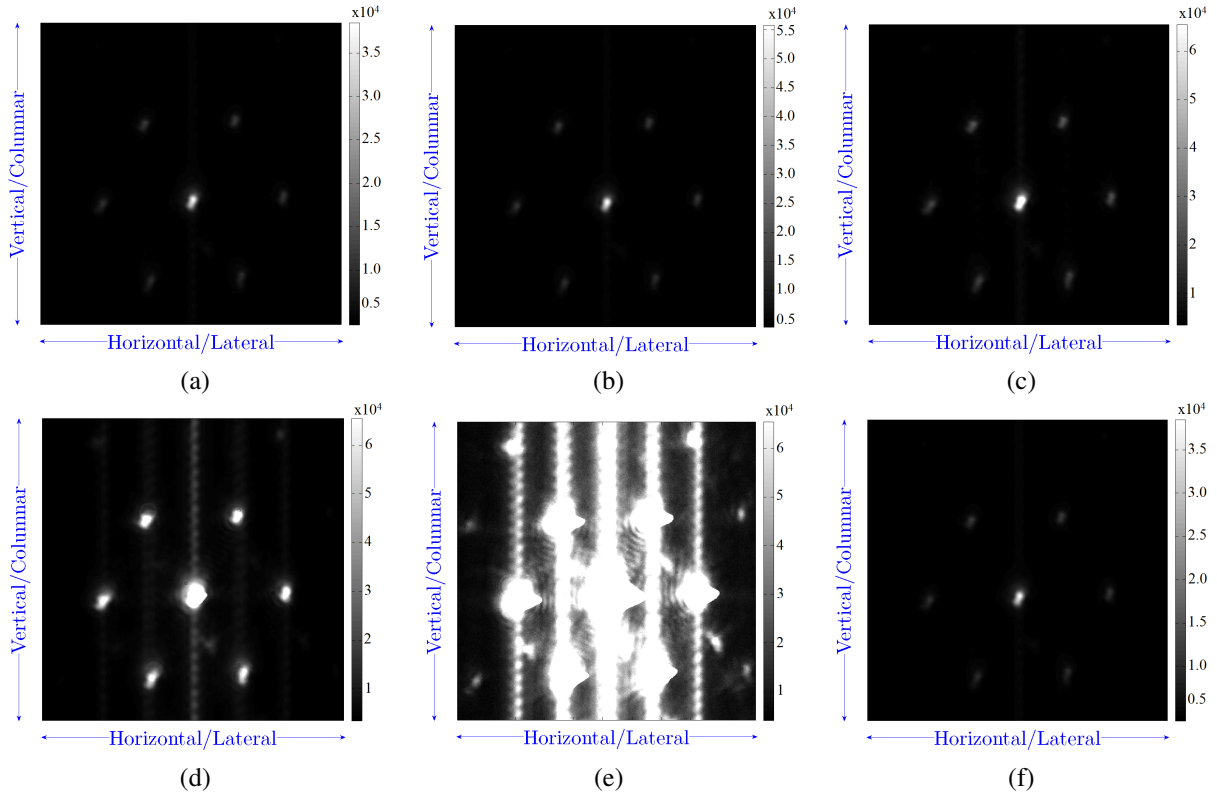

Fig 6 A science image from the NCB. The exposure time was set to 1.7ms. The four images above were captured at different gains. (a) An image with gain set to No Gain. (b) An image with gain set to (approx) 1.5 (c) An image with gain set to (approx) 5 (d) An image with gain set to (approx) 10 (e) An image with gain set to Max 1000. (f) The image in (a) re-produced next to (e) to help comparison. The images evolve from just a point source, visible in (a) to a blooming and saturated mess in (e). However, note in (e) that thanks to the amplifying power of an EMCCD the speckle pattern has become highly pronounced. It is this ability to amplify low-light details that makes the EMCCD so important to instruments that will image exoplanets . In (e) another form of blooming, only seen in an EMCCD, is introduced – horizontal blooming. Horizontal blooming is caused by charge transfer inefficiencies in the multiplication register. The very large amount of charge generated by a star – at maximum magnification – generates an even larger amount of multiplied charge. This large amount of multiplied charge does not transfer very efficiently through a register chain. Some charge from the very bright pixels tends to get trapped and released into pixels that follow, as the image is clocked out of the sensor. This produces a streaking effect in the image. Images are from the GSFC lab test bed and not an actual starlight image.

image that are not a result of integration of light. These artifacts do not appear in images produced by CMOS or CCD devices. The artifacts distort the Airy pattern of the star and cannot be corrected with a coronagraphic instrument's active wavefront control system. As such they make a coronagraphic system unusable for high-contrast imaging. Maturing imaging (readout) techniques for an EMCCD can alleviate these problems and make it possible/easier to implement high-contrast imaging in a coronagraph with a high-gain sensor.

4 Imaging Techniques for an EMCCD in a CGI

Modern EMCCD based cameras have demonstrated multiplication factors as high as 5000,[72] by cooling the sensor, experimenting with different clocking modes and creating very smooth high-voltage clock signals. However, these demonstrations have been carried out with low dynamic range scenes. When a bright source appears next to a dim source in a scene, it has been shown here (Section 3) that the multiplication stage might obscure the dim signal with a blooming artifact. In the WFIRST coronagraph a field-stop-like focal plane will be used to prevent bright stellar light from reaching the detector. However, this field stop might be detrimental to disk science and it is not clear yet if all observations will be carried out using it. A field stop is also likely to complicate wavefront control in a coronagraph. It is also not clear whether the full focal-plane will be used for imaging the star-planet system. Charge transfer inefficiencies might require placement of the star very near the readout registers. Similarly for the Integral Field Spectrometer (IFS), masking of the outer portions of the shaped pupil coronagraph (SPC) will be a compromise between discovery space and leakage

of the exterior PSF. Wherever the PSF leaks through the hard stop masking, trailing will occur at varying levels, some of which may impact final SNR.[26] In this section, techniques will be discussed that address the problems of starlight saturation and blooming. These steps are key to using an EMCCD in a high-contrast planet finder instrument. Here are three ways to use an EMCCD in a CGI:

4.1 Suppressing Horizontal Charge Blooming in a CGI with Solid State Circuits

A purely silicon based implementation from On-Semiconductors of an algorithm to prevent charge blooming because of uniform multiplication across an image has already been demonstrated.[73] In this implementation a decision making circuit channels high-signal pixels out of the chip through a regular CCD amplifier. Low-signal pixels are channeled through a second amplifier after being amplified in an electron multiplication stage. This method has the advantage of producing variable gain at a pixel level and permits nulling in a full circle around a star. However, it produces a very small amount of gain (60x) and has a finite lifetime – because of the way in which it handles excess charge. Because photon-counting imaging cannot be achieved with low-gain EMCCDs – it is unlikely that this sensor will replace an e2v CCD 201 as a photon-counting sensor for astrophysics in the foreseeable future.

e2v has produced a new sensor to address the issue of horizontal blooming.[74] A charge drain has been inserted in the multiplication register to bleed excess charge. Initial results have been promising. Unlike the new EMCCD from On-semiconductors this sensor can generate a large amount of gain (x1000). However, the sensor does not have a CCD signal path and like the On-Semiconductor sensor has a very small full well (20ke$^-$). These sensors are primarily designed to bleed excess charge generated by cosmic ray hits.

Variable Gain Imaging with an EMCCD as a means for suppressing horizontal blooming is an open topic of research. The method proposed here is the only known alternative. In addition, the method proposed here is the only way to preserve dynamic range and suppress horizontal charge blooming, simultaneously. Therefore, despite the new advances in CCD solid state circuits inside new and novel EMCCDs, the clocking scheme presented next is still very relevant.

4.2 Suppressing Horizontal Charge Blooming in a CGI with a Variable Multiplication Gain Clock

Since starlight is very bright and planet light is very dim – amplifying the starlight at the same rate as the planet light would corrupt the image by introducing horizontal blooming. A mechanism to amplify different sections of the image with different gains is therefore proposed and is called "Variable Multiplication Gain Clocking." Variable multiplication gain imaging is achieved by clocking the rows of the image that contain the central peak and six side lobes with less or no charge multiplication – This is achieved by reading out the specific rows through the standard CCD amplifier or through the multiplication register at very-low or no gain. The rows of the image that contain only speckle and the planet can be read-out in high-gain mode through the multiplication register. The architecture of an e2v EMCCD is shown in Fig. 1. A variable multiplication gain clock will eliminate the "saturation" and "horizontal blooming" problems associated with high-contrast imaging. This method does suffer from a drawback. It operates in a row-parallel architecture (all pixels in a row must be amplified at the same level) and therefore makes nulling in a full circle around the star impossible.

Variable gain signal processing is very common in CMOS sensors. Smart CMOS sensors can implement this function on the focal plane itself.[75] However, signal processing circuits are never embedded inside a CCD. Signals must be processed during the read-out phase or outside the detector by an external device. Processing different sections of a focal plane with different spatial filter operators using an analog mode external image processor has been demonstrated by a neural signal processing group.[76] A different implementation where the focal plane is filtered with different operators at a global level using an external processor has also been demonstrated.[77] This program is therefore proposing to extend to an EMCCD camera for astronomical systems what CMOS groups have already done for intelligent cameras in robotic systems.

The image in Fig. 6a was amplified in software and the results are shown in Fig. 7. This simulation amplified the entire image with an addition operator. The speckle pattern becomes as visible in this image as seen in Fig. 6e. Amplification using a variable gain clock was also simulated and the results are shown in Fig. 8 and Fig. 9. Speckle pattern in Fig. 9 is seen to be amplified to level as high as seen in Fig. 7 and Fig. 6e. Figure 8 provides evidence that variable gain signal processing can prevent starlight saturation and horizontal blooming in an EMCCD. The enlargement of the central region is caused by higher photon-counts near the star, that causes the region to appear very bright and/or saturated in this amplified image. However, this is not a blooming artifact and can be suppressed with starlight suppression algorithms. These very elementary simulations of variable gain imaging show that the star and the speckles can be amplified with different gains to produce a scene that can be used to perform high-contrast imaging in small IWA of a coronagraph. This is not a perfect simulation because in a real coronagraph the amplification function will not take the

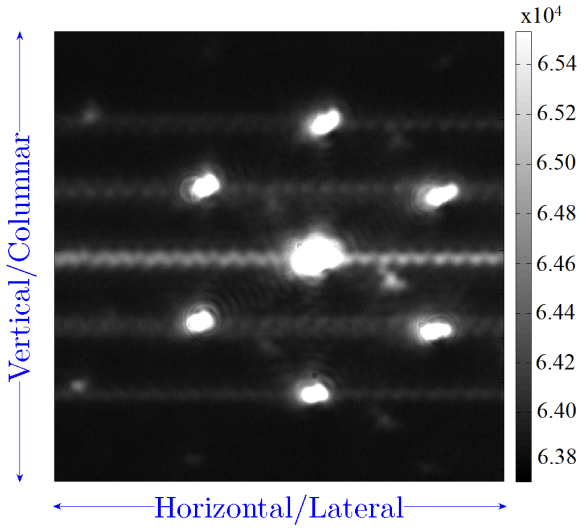

Fig 7 This image was created in software with an addition operation on a transposed version of the image in Fig. 6a. This amplifies the stellar and specke signals equally. The speckle pattern is nearly amplified to levels seen in Fig. 6e. The absence of blooming in this image is evidence that a large part of image corruption in Fig. 6e is caused by blooming, and that blooming is caused by the multiplication process that can be suppressed by variable gain imaging.

form of a step function, as shown here. Instead, amplification will have a wave-like distribution, peaking between

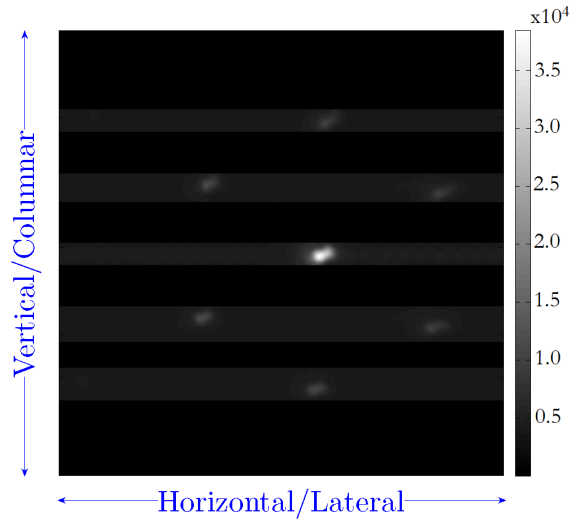

Fig 8 This image and the following image were artificially generated in software from the image in Fig. 6a. The image in Fig. 6a was transposed and used as the base image for this simulation. An addition operation was performed on the base image to amplify its signal in the rows that do *not* contain the central peak or the six side lobes (simulating variable gain imaging). The image above shows the rows of the amplified image that contain the central peak and the six side lobes. It contains no evidence of blooming. The central peak and side-lobes are not saturated.

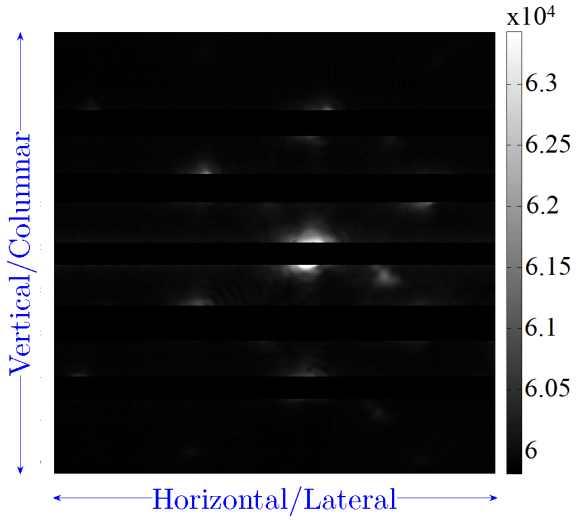

Fig 9 This image shows rows of the simulated image that contain amplified speckle pattern. It contains no blooming artifact! Both sides of the central peak are available for suppressing starlight and imaging exoplanets – resolving the problem created by horizontal blooming in Fig. 6e.

the side lobes and the star and approaching unity at the star and the side lobes. This function in addition will not be static during a high-contrast experiment. It will be dynamically modified as starlight is suppressed and nulling is implemented. The three images here are meant solely as an example of variable gain imaging in a high-contrast instrument. More realistic images will become available when this camera is inserted in a high-contrast instrument.

4.3 Suppressing Horizontal Charge Blooming in a CGI with a Mask

Third, a partially transparent petal-shaped mask[78] can be used in the science channel to partially block the starlight and prevent blooming and saturation. However, it should be noted that a mask in the science channel of a nulling type coronagraph will introduce its own particular diffraction pattern and modify the speckle distribution. Therefore, a mask should only be used after carefully modelling its effect in the instrument.

5 A New Controller for an EMCCD in a CGI – Presenting A Case

NASA commissioned a study in 2006 to derive requirements for a space based planet finder camera. The final report from this study produced basic, system-level, requirements for such a camera[40]. The study identified a photon-counting L3-CCD from Teledyne e2v as the most likely detector in a visible wavelength CGI. In 2016, a full analysis of the WFIRST telescope's, coronagraph and camera system,[79] revealed that existing clocking and

readout techniques will make it extremely difficult to image an exoplanet with an EMCCD. WFIRST proposes to address the problems by positioning the stellar peak away from the focal plane and using focal plane field stops. It has been shown here that the same problems can be easily solved electronically by modifying the clocking scheme of the EMCCD. A commercially available EMCCD controller cannot implement these novel schemes. A new controller to effectively use an EMCCD based camera in a CGI was therefore called for. Herein we will discuss some of the design considerations for such a controller.

An interferometric coronagraph operates its science camera with two competing purposes. First – it is used to implement fine wavefront control algorithms that create a "dark hole (null)" around the star. To do this, the control algorithm uses an image of the star-planet system created through a high-resolution Analog-to-Digital Converter (ADC). Second – the science camera images an exoplanet in the "dark hole around the star" in photon counting mode. Photon-counting imaging traditionally uses a thresholding[49,80] technique to report the presence of a photon at a given pixel. This is a binary reporting scheme – A pixel that detects a photon, signals a high-logic level to its processor (regardless of the number of photons) and pixels that do not detect a photon, signal a low logic-level to the processor. No attempt is made to measure the energy of the photon or the number of photons incident on the pixel. A camera that can perform both these operations – photon-counting and digitization mode imaging – in two different regions of the sensor, inside a single frame has not been reported. A dual mode imaging controller is critical for an EMCCD in a coronagraphic instrument.

A new testbed for EMCCD controllers was initiated at GSFC in 2013 to implement the techniques that have been discussed in this report (Section 4). This was in direct response to the failure of a commercial EMCCD based camera, in the VNC, in 2012 (Section 3). A Digital-to-Analog Converter (DAC) and Field Programmable Gate Array (FPGA) based shaped clock generator system was selected that is capable of producing smooth clock signals for an e2v, 512×512 CCD-97 EMCCD detector at 6.5MHz/20fps. Higher-speed clocks are possible, but these clocks do not maintain smoothness. An FPGA based System was chosen because NASA considers them to be easier to convert to space based systems. A DAC-based shaped clock circuit was chosen because these circuits can generate arbitrarily shaped clocks. Shaped clock circuits can control the transition time of a clock signal and are primarily used to reduce Clock Induced Charge (CIC). CIC is a phenomenon where energy from a read-out clock knocks out electrons from the lattice structure and introduces them to the imaging chain as photo-electrons, i.e. these electrons behave like photoelectrons but are not a result of integration of light. At very low light levels, CIC becomes the dominant source of background noise in an EMCCD. While CIC is caused by all clocks,[10] the multiplication clock has the effect of both introducing CIC and of amplifying CIC introduced by other clocks. A multiplication clock's amplitude has a direct correlation to CIC – lower amplitudes produce less CIC. An EMCCD is therefore operated at low-temperatures (Figure 10), because at lower temperatures, a lower amplitude multiplication clock produces the same gain as a higher amplitude multiplication clock, without generating additional CIC.

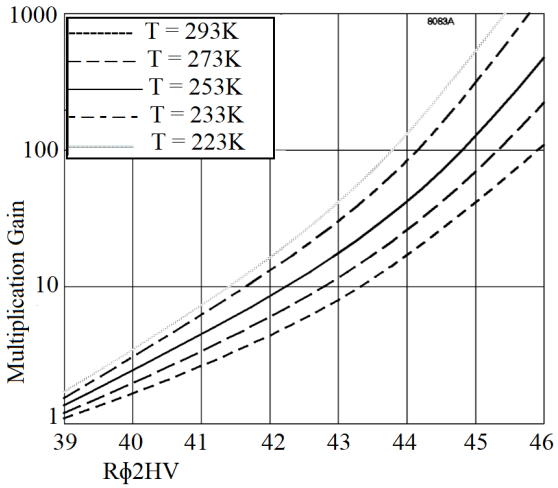

Fig 10 This plot (re-produced with permission from Teledyne e2v) shows the dependence of Multiplication Gain (y-axis) on the amplitude of the Multiplication Gain Clock (RϕHV – x-axis), at different temperatures. An EMCCD produces more gain at lower temperatures with the same multiplication clock (amplitude) than at higher temperatures. CIC is not directly related to temperature. It is, however, directly proportional to the amplitude of the multiplication clock. An EMCCD, therefore, produces the same gain with less CIC at lower temperatures, than at higher temperatures, because it uses a smaller amplitude multiplication clock.

The GSFC testbed in future will be used to test high-speed DACs (≈GHz) that will test high-speed photon-counting with an EMCCD in space. The GSFC controller for EMCCDs uses a 210MHz DAC to generate smooth CCD clock signals. At high clock rates the noise content in any image sensor's output increases considerably. Photon-counting imaging is expected to be very difficult at high clock speeds.[81] Literature on photon-counting with EMCCDs, do not cite a maximum clock speed at which true photon-counting becomes impossible. In a coronaraph, a high-speed camera is desirable because it allows a space based system to reject spurious events caused by cosmic rays. A low-light system in space and even on the ground systems tends to be susceptible to cosmic ray events. Scanning a low-light detector array at a high-rate is one of the ways to flag cosmic ray hits. Polling cosmic ray events is a major task when a low-light

and single photon counting cameras are used for astronomical imaging. A higher-speed camera also condenses data collection time. This is an important consideration when designing an astronomical imaging system. Ground telescope systems operate only during a few hours of the night. Space systems being few and far between in number are highly over-subscribed. Instruments for astronomical observations are therefore always looking for ways to speed up data acquisition – even in a 24hr space environment. A high-speed camera is therefore always desirable.

Furthermore, it has also been shown that post processing algorithms perform much better, even adding an order of magnitude to an instrument's contrast-ratio, when they can extract multiple images from a high-contrast instrument without modifying its deformable mirror's setting.[82,83] (An MMA corrects wave-front drifts caused by environmental factors on a space based system). A fast camera can capture more images between control loops than a slow camera without effecting wavefront. An analysis of frame rate vs. camera resolution vs. stability vs. contrast sensitivity isn't available for the VNC. However, such an analysis was reported for the JPL/HCIT in 2015[84] and it confirms that higher speed control produces higher contrast. A higher-speed camera is therefore, again, highly desirable out of reasons of mathematical and analytical necessity.

"Frame-rate" should not be confused with "Integration time". There are two ways to image an exoplanet with a photon-counting camera. Both can make use of high frame rate readout. The first is with short-exposure astronomy and second with long-exposure astronomy. In short exposure astronomy, the integration time of a camera is set very low and a system depends on luck to capture the single-photon arrival from an exoplanet. This method has the advantage of collecting very few photons from the star. However, capturing the planetary photon is also not guaranteed. In long exposure astronomy integration time is increased to be longer than the inter-arrival time of single-photons from exoplanets. This adds more certainty to the single-photon capture process. However, it also increases the number of photons received from the parent star. As a result the chances of blooming and saturation are also higher. In the case of short exposure astronomy, variable multiplication gain imaging might or might not be required. In the case of long exposure astronomy variable multiplication gain imaging is imperative. Which mode is most suitable for imaging an exoplanet? An answer to that a question is not available at this time.

An Teledyne e2v L3 EMCCD was selected as an imaging sensor for a CGI long before high-contrast experiments had been carried out with one. Imaging artifacts and electronic methods for removing them (in the form of Variable Multiplication Gain Imaging), the need for dual mode imaging, and the potential need for high-speed photon-counting – all present a need for a new controller for EMCCDs.

6 High-Contrast Imaging with an EMCCD in a CGI – A Roadmap for the Future

These are the first results from experiments in high-contrast imaging with an EMCCD in a coronagraphic instrument. The new results presented in this report are *three folds*.

First, two major problems in high-contrast imaging with EMCCD detectors – starlight saturation and starlight blooming – are identified and presented. These problems are demonstrated with images taken with an EMCCD camera in an interferometric optical system.

Second, a solution for horizontal blooming and starlight saturation with a new way of clocking EMCCDs – Variable Multiplication Gain Imaging – is proposed. Simulations of images that would arise from this new way of clocking an EMCCD are presented.

Third, and finally, an electronics package for clocking an EMCCD in a high-contrast instrument in variable gain photon-counting mode is presented. A firmware package for this electronics bundle has also been developed. Analog signal processing circuits will be developed in the future to process images from a high-contrast instrument with this system.

It is expected that caliberation of this camera, once built, will be a major undertaking. In this report, only problems arising from high-intensity imaging were discussed. A whole set of problems arising from lowlight/photon-counting and high-contrast imaging – like linearity, noise, scattered light, charge transfer inefficiencies, its variation with temperature – are not discussed. It is expected that these and other problems will make calibration of this camera and its use in a coronagraph a major challenge.

Over the next few years, this new controller will be used to conduct dual mode imaging – photon-counting and digitization – experiments with an EMCCD in a high-contrast instrument. Three future milestones for this camera are as follows: A demonstration of photon-counting and variable multiplication gain imaging. A demonstration of starlight suppression. A demonstration of high-contrast imaging. It is expected that these experiments, and other ideas presented in this paper, will eliminate the need for field stop mechanisms in future EMCCD based high-contrast, photon-counting focal plane assemblies and demonstrate starlight suppression and high-contrast photon-counting imaging using electronic means, exclusively. These techniques are not yet perfect. However, removing the field stop, using a full sensor for observations, using high-speed clocks, using variable multiplication gain clocks, using complex readout techniques to scan an EMCCD array in multiple modes – within a single

frame – will allow observation of a full star-planet-disk system simultaneously. This will considerably increase the amount of stellar, disk and exoplanet science returned from future missions in space than will be returned by the current mission profile of the WFIRST coronagraph.

This system will be a significant advancement in the art and will substantially increase the quantity and quality of science acquired by missions to directly image exoplanets in space.

Acknowledgments

The authors acknowledge the GSFC Internal Research and Development program for funding Udayan Mallik's work on the VNC's computer, camera and optical systems and Dominic Benford's work on galaxy survey telescopes. Authors acknowledge the Strategic Astrophysics Technology/Technology Demonstration for Exoplanet Mission programme office for supporting Peter Petrone. The authors, also acknowledge that Fig.1 and 10, were generated at Teledyne e2v and that Teledyne e2v permitted their use in this publication. Finally, they thank the reviewers of this paper for their comments and feedback.

References

1 S. S. Board, *New worlds, new horizons in astronomy and astrophysics*, National Academies Press, New York (2011).

2 M. Clampin, R. Lyon, P. Petrone, *et al.*, "Visible nulling coronagraph technology maturation: High contrast imaging and characterization of exoplanets," in *Technology Demonstration for Exoplanet Mission, Milestone 1, JPL Document D-80950*, (2013).

3 B. Hicks, M. Bolcar, R. Lyon, *et al.*, "Achromatic visible nulling coronagraph technology maturation," in *Technology Demonstration for Exoplanet Mission, Milestone 3, JPL Document D-1547413*, (2016).

4 B. Hicks, M. Bolcar, P. Petrone, *et al.*, "Nulling of an actively-controlled segmented aperture telescope," in *Technology Demonstration for Exoplanet Mission, Milestone 3 Whitepaper, JPL Document D-1549543*, (2016).

5 M. Bolcar, "Next generation visible nulling coronagraph," in *Technology Demonstration for Exoplanet Mission, Abstract*, (2014).

6 G. Serabyn, J. Trauger, D. Moody, *et al.*, "Technology milestone report – vortex coronagraph technology," in *Technology Demonstration for Exoplanet Mission, Milestone 1, JPL Document D-92350*, (2014).

7 O. Guyon, B. Kerr, A. Kuhnert, *et al.*, "Phase-induced amplitude apodization (piaa) technology, 10% bandpass contrast demonstration," in *Technology Demonstration for Exoplanet Mission, Milestone 3, JPL Document D-93064*, (2014).

8 J. Trauger, B. Gordon, J. Krist, *et al.*, "Hybrid lyot coronagraph technology - linear masks," in *Technology Demonstration for Exoplanet Mission, Milestone 3, JPL Document D-78698*, (2012).

9 U. Mallik, R. Lyon, D. Benford, *et al.*, "Maturing ccd photon counting technology for space flight," in *Techniques and Instrumentation for Detection of Exoplanets VII.*, *Proc. of SPIE* (2015).

10 Y. Wen, B. Rauscher, R. Baker, *et al.*, "Individual photon counting using e2v l3 ccds for low background astronomical spectroscopy," in *Astronomical Telescopes and Instrumentation*, *International Society for Optics and Photonics*, 716–731 (2006).

11 P. Szypryt, B. Mazin, B. Bumble, *et al.*, "Ultraviolet, optical, and near-ir microwave kinetic inductance detector materials developments," *IEEE Transactions on Applied Superconductivity* (2015).

12 P. Verhoeve, D. D. E. Martin, R. A. Hijmering, *et al.*, "S-Cam 3: Optical astronomy with a STJ-based imaging spectrophotometer," *Nuclear Instruments and Methods in Physics Research A* **559**, 598–601 (2006).

13 M. R. Bolcar, L. Feinberg, K. France, *et al.*, "Initial technology assessment for the large-aperture uv-optical-infrared (luvoir) mission concept study," *Proc. of SPIE* **9904**, 9904 – 9904 – 12 (2016).

14 J. E. Krist, G. F. Hartig, M. Clampin, *et al.*, "Advanced camera for surveys coronagraph on the hubble space telescope," *Proc.SPIE* **4860**, 4860 – 4860 – 12 (2003).

15 J. J. Green, C. Beichman, S. A. Basinger, *et al.*, "High contrast imaging with the jwst nircam coronagraph," *Proc. SPIE* **5905**, 5905–5905–11 (2005).

16 E. Artigau, "Niriss aperture masking interferometry: an overview of science opportunities," in *Space Telescopes and Instrumentation 2014: Optical, Infrared, and Millimeter Wave*, *SPIE proc* **9143** (2014).

17 A. Boccaletti, P. Riaud, J. Baudrand, *et al.*, "Exoplanet imaging at mid-ir wavelengths with jwst," *In Earths: DARWIN/TPF and the Search for Extrasolar Terrestrial Planets* (2003).

18 R. Lyon, M. Clampin, P. Petrone, *et al.*, "Vacuum nuller testbed (vnt) performance, characterization and null control: progress report.," in *SPIE Optical Engineering+ Applications*, *Proc. SPIE*, 716–731 (2011).

19 J. Y. Tang and K. Hess, "Impact ionization of electrons in silicon (steady state)," *Journal of applied physics* **54(9)**, 5139–5144 (1983).

20 "Em n2 1024 specsheet," This document is available at http://www.nuvucameras.com/wp-content/uploads/2016/12/NüVüCaméras-EM-N2-1024.pdf.

21 "e2v ccd 201 spec sheet," This document is available at https://www.e2v.com/shared/content/resources/File/documents/Imaging 2017/EM Sensors/CCD201-20/1491.pdf.

22 S. Nikzad, M. Hoenk, A. Jewell, *et al.*, "Single photon counting uv solar-blind detectors using silicon and iii-nitride materials," *Sensors* **16**(6), 927 (2016).

23 M. R. Bolcar, K. Balasubramanian, J. Crooke, *et al.*, "Technology gap assessment for a future large-aperture ultraviolet-optical-infrared space telescope," *Journal of Astronomical Telescopes, Instruments, and Systems* **2**(4), 041209–041209 (2016).

24 B. J. Rauscher, E. R. Canavan, S. H. Moseley, *et al.*, "Detectors and cooling technology for direct spectroscopic biosignature characterization," in *Journal of Astronomical Telescopes, Instruments, and Systems*, **2**(4), 041212–041212 (2016).

25 O. Djazovski, O. Daigle, D. Laurin, *et al.*, "Electron-multiplying ccds for future space instruments," in *In Photonics North 2013*, *International Society for Optics and Photonics*, 89150Q–89150Q (2013).

26 J. H. Debes, M. Ygouf, E. Choquet, *et al.*, "Wide-field infrared survey telescope – astrophysics focused telescope assets coronagraphic operations: lessons learned from the hubble space telescope and the james webb space telescope," in *Journal of Astronomical Telescopes, Instruments, and Systems*, **2** (2015). http://dx.doi.org/10.1117/1.JATIS.2.1.011010.

27 M. Levine and D. Mawet, "Overview of technologies for direct optical imaging of exoplanets," in *The Astronomy and Astrophysics Decadal Survey*, *Technology Development Papers, NASA*(37), 1–11 (2009).

28 S. Shaklan, M. Levine, M. Foote, *et al.*, "The afta coronagraph instrument," in *In SPIE Optical Engineering+ Applications*, *International Society for Optics and Photonics* (2013).

29 R. Lyon and M. Clampin, "Space telescope sensitivity and controls for exoplanet imaging," in *In SPIE Optical Engineering*, **51**(1) (2012). 011002-1.

30 A. Dressler, *Origins 2003: Roadmap for the Office of Space Science Origins Theme*, Diane Pub Co. (2003).

31 M. Shao, S. Bairstow, B. Levine, *et al.*, "Davinci, a diluter aperture visible nulling coronagraphic instrument," in *In SPIE Astronomical Telescopes+ Instrumentation*, *International Society for Optics and Photonics* (2008).

32 M. Levine, D. Lisman, S. Shaklan, *et al.*, "Terrestrial planet finder coronagraph (tpf-c) flight baseline concept," in *arXiv preprint arXiv:0911.3200*, (2009).

33 B. J. Makins, "Interferometer architecture trade studies for the terrestrial planet finder mission," in *Doctoral dissertation, Massachusetts Institute of Technology*, (2002).

34 M. Clampin, R. Lyon, G. Melnick, *et al.*, "The extrasolar planetary imaging coronagraph: Architectures of extrasolar systems," in *ASMC Study Report*,

35 K. C. France, "The luvoir science and technology definition team (stdt): overview and status," in *In SPIE Astronomical Telescopes+ Instrumentation*, *International Society for Optics and Photonics* (2016).

36 K. Stapelfeldt, R. Belikov, G. Bryden, *et al.*, "Exo-c imaging nearby worlds final report," Available at https://exoplanets.nasa.gov/exep/studies/probe-scale-stdt/.

37 S. Seager, W. Cash, S. Domagal-Goldman, *et al.*, "Exo-s: starshade probe-class exoplanet direct imaging mission concept final report," (2015).

38 L. K. Harding, R. T. Demers, M. Hoenk, *et al.*, "Technology advancement of the ccd201-20 emccd for the wfirst coronagraph instrument: sensor characterization and radiation damage," in *Journal of Astronomical Telescopes, Instruments, and Systems*, **2**(1), 011007–011007 (2016).

39 B. A. Mazin, P. Day, H. LeDuc, *et al.*, "Superconducting kinetic inductance photon detectors," in *In Astronomical Telescopes and Instrumentation*, (2002).

40 M. Clampin, R. Lyon, L. Petro, *et al.*, "Coronagraphic exploration camera (corecam)," in *Proc. SPIE 6265, Space Telescopes and Instrumentation I: Optical, Infrared, and Millimeter*, (2006). doi:10.1117/12.672816; http://dx.doi.org/10.1117/12.672816.

41 G. Pilbratt, J. Riedinger, T. Passvogel, *et al.*, "Herschel space observatory-an esa facility for far-infrared and submillimetre astronomy," in *Astronomy and Astrophysics*, (2010).

42 J. Tauber, N. Mandolesi, J. Puget, *et al.*, "Planck prelaunch status: The planck mission," (2010).

43 O. Daigle, P.-O. Quirion, and S. Lessard, "The darkest emccd ever," in *SPIE Astronomical Telescopes + Instrumentation*, *International Society for Optics and Photonics*, 774203–774203 (2010).

44 D. Spergel, N. Gehrels, J. Breckinridge, *et al.*, "Wide-field infrared survey telescope-astrophysics focused telescope assets wfirst-afta final report," *arXiv preprint arXiv:1305.5422* (2013).

45 J. C. Green, "The cosmic origins spectrograph," *International Society for Optics and Photonics* , 352–359 (2000).

46 S. Nikzad, M. E. Hoenk, F. Greer, *et al.*, "Delta-doped electron-multiplied ccd with absolute quantum efficiency over 50% in the near to far ultraviolet range for single photon counting applications," *Applied Optics* **51**(3), 365–369 (2012).

47 C. Mackay, T. D. Staley, D. King, *et al.*, "High-speed, photon-counting ccd cameras for astronomy," in *In SPIE Astronomical Telescopes+ Instrumentation*, *International Society for Optics and Photonics*, 774202–774202 (2010).

48 C. D. Mackay, "Near diffraction limited visible imaging on 10 m class telescopes with emccds," in *In Scientific detectors for astronomy*, *Springer Netherlands*, 93–98 (2005).

49 O. Daigle, J. L. Gach, C. Guillaume, *et al.*, "Cccp: a ccd controller for counting photons," in *SPIE Astronomical Telescopes + Instrumentation*, *International Society for Optics and Photonics*, 70146L–70146L (2008).

50 "Low light technical note 4 dark signal and clock induced charge in l3vision^{TM} ccd sensors," in *e2v Systems Technical Notes*, (2015).

51 O. Daigle, O. Djazovski, D. Laurin, *et al.*, "Characterization results for extreme low-light imaging," in *SPIE Astronomical Telescopes + Instrumentation*, *International Society for Optics and Photonics*, 845303–845303 (2012).

52 O. Daigle, O. Djazovski, J. Dupois, *et al.*, "Astronomical imaging with emccds using long exposures," in *Proc of SPIE 9154, High Energy Optical and Infrared Detectors for Astronomy VI*, *International Society for Optics and Photonics* **9154D** (2014). [doi:10.1117/12.2056617].

53 O. Daigle, J.-L. Gach, C. Guillaume, *et al.*, "L3ccd results in pure photon-counting mode," in *In SPIE Astronomical Telescopes+ Instrumentation*, *International Society for Optics and Photonics*, 219–227 (2004).

54 A. G. Basden, C. A. Haniff, and C. D. Mackay, "Photon counting strategies with low-light-level ccds," in *Monthly notices of the royal astronomical society 345*, (3), 985–991 (2003).

55 M. S. Robbins and B. J. Hadwen, "The noise performance of electron multiplying charge-coupled devices," in *IEEE Transactions on Electron Devices*, **50**(5), 1227–1232 (2003).

56 J. Hynecek and T. Nishiwaki, "Excess noise and other important characteristics of low light level imaging using charge multiplying ccds," in *IEEE Transactions on Electron Devices*, **50**(1), 239–245 (2003).

57 B. Li, Q. Song, J. Jin, *et al.*, "Circuit design of an emccd camera," *International Society for Optics and Photonics*, 84532O–84532O (2012).

58 S. Tulloch, *Astronomical Spectroscopy with Electron Multiplying CCDs*, Department of Physics and Astronomy The University of Sheffield, Dissertation in Candidature for the Doctor of Philosophy (2010).

59 R. Lyon, M. Clampin, P. Petrone, *et al.*, "High contrast vacuum nuller testbed (vnt) contrast, performance, and null control," in *SPIE Astronomical Telescopes+ Instrumentation*, *Proc. SPIE*, 716–731 (2012).

60 R. Lyon, M. Clampin, M. Shao, *et al.*, "Nulling coronagraphy for exo-planetary detection and characterization," in *IAU Colloquium No. 200, Direct Imaging of Exoplanets: Science and Techniques*, C. Aime and F. Vakili, Eds., 716–731 (2005).

61 B. M. Levine, M. Shao, D. T. Liu, *et al.*, "Planet detection in visible light with a single aperture telescope and nulling coronagraph," *Optical Science and Technology, SPIE's* 48^{th} *Annual Meeting.* , 200–208 (2003).

62 M. Clampin, G. Melnick, R. Lyon, *et al.*, "Extrasolar planetary imaging coronagraph(epic)," *SPIE Astronomical Telescopes+ Instrumentation. International Society for Photonics* , 62651B–62651B (2006).

63 R. Samuele, J. K. Wallace, E. Schmidtlin, *et al.*, "Experimental progress and results of a visible nulling coronagraph.," in *Aerospace Conference, 2007 IEEE*, 1–7 (2007).

64 E. S. Douglas, C. B. Mendillo, B. Hicks, *et al.*, "Status of the picture sounding rocket to image the epsilon eridani circumstellar environment," in *American Astronomical Society Meeting Abstracts*, **224** (2014).

65 N. Murakami, K. Yokochi, J. Nishikawa, *et al.*, "Polarization interferometric nulling coronagraph for high-contrast imaging," in *Applied optics*, **49**, D106–D114 (2010).

66 R. G. Lyon, B. Hicks, M. Clampin, *et al.*, "Phase-occultation nulling coronagraphy," *arXiv preprint arXiv:1504.05747* .

67 S. Tulloch and Q. C. Miranda in *Technical Note 1: Introduction to EMCCDs*, (2009).

68 T. J. Fellers and M. W. Davidson, "Concepts in digital imaging technology - ccd saturation and blooming," http://hamamatsu.magnet.fsu.edu/articles/ccdsatandblooming.html.

69 "Ccd blooming and anti-blooming," This article is available at http://www.andor.com/learning-academy/ccd-blooming-and-anti-blooming-the-principle-of-blooming.

70 P. Fereyre and G. Powell, "Cmos image sensors are entering a new age," *e2v System Content Uploads* .

71 D. J. Denvir and E. Conroy, "Electron-multiplying ccd: the new iccd," in *International Symposium on Optical Science and Technology*, *International Society for Optics and Photonics*, 164–174 (2003).

72 O. Daigle, C. Carignan, and S. Blais-Ouellette, "Faint flux performance of an emccd," in *Astronomical Telescopes and Instrumentation*, *International Society for Optics and Photonics*, 62761F–62761F (2006).

73 C. Parks, S. Kosman, E. Nelson, *et al.*, "A 30 fps 1920 1080 pixel electron multiplying ccd image sensor with per-pixel switchable gain," *In International Image Sensor Workshop (IISW)* , 8–11 (2015).

74 O. Daigle, J. Turcottea, E. Artigau, *et al.*, "Preliminary characterization results of a large format 4k x 4k emccd," in *Proc. of SPIE High Energy, Optical, and Infrared Detectors for Astronomy VIII*, (10709) (2018).

75 Y. M. Chi, U. Mallik, E. Choi, *et al.*, "Cmos pixel-level adc with change detection," in *In Circuits and Systems, 2006. Proceedings. 2006 IEEE International Symposium on,*, *Proc. of ISCAS* (2006).

76 R. J. Vogelstein, U. Mallik, E. Culurciello, *et al.*, "Spatial acuity modulation of an address-event imager," *Proceedings of the 11th IEEE International Conference on Electronics, Circuits and Systems* , 207–210 (2004).

77 U. Mallik, R. J. Vogelstein, E. Culurciello, *et al.*, "A real-time spike-domain sensory information processing system," *IEEE Intl. Symposium for Circuits and Systems* , 1919–1922 (2005).

78 S. Shiri and W. Wasylkiwskyj, "Poisson-spot intensity reduction with a partially transparent petal-shaped optical mask," in *Journal of Optics*, **15** (2013).

79 W. A. Traub, J. Breckinridge, T. P. Greene, *et al.*, "Science yield estimate with the wide-field infrared survey telescope coronagraph," in *Journal of Astronomical Telescopes, Instruments, and Systems*, **2** (2016).

80 U. Mallik, M. Clapp, E. Choi, *et al.*, "Temporal change threshold detection imager," *IEEE International Digest of Technical Papers for Solid State Circuits Conference* (2005).

81 O. Daigle, O. Djazovski, M. Francoeur, *et al.*, "Emccds: 10mhz and beyond," in *SPIE Astronomical Telescopes + Instrumentation*, *International Society for Optics and Photonics*, 91540B–91540B (2014).

82 M. Ygouf, L. Pueyo, R. Soummer, *et al.*, "Data processing and algorithm development for the wfirst-afta coronagraph: reduction of noise free simulated images, analysis and spectrum extraction with reference star differential imaging," in *In SPIE Optical Engineering+ Applications*, *International Society for Optics and Photonics* (2015).

83 M. Ygouf, N. T. Zimmerman, L. Pueyo, *et al.*, "Data processing and algorithm development for the wfirst coronagraph: comparison of rdi and adi strategies and impact of spatial sampling on post-processing," in *In SPIE Astronomical Telescopes+ Instrumentation*, *International Society for Optics and Photonics* (2016).

84 E. Sidick, S. Shaklan, and K. Balasubramanian, "Hcit broadband contrast performance sensitivity studies," in *In SPIE Optical Engineering+ Applications*, *International Society for Optics and Photonics* (2012).

Udayan Mallik was a US Civil Servant at the NASA, Goddard Space Flight Center. Between 2010 and 2016, he was a member of the Visible Nulling Coronagraph Group where he developed computer, detector, software, electronic systems for the instrument. He was Principal Investigator of a program that investigated High-Contrast Imaging with a photon-counting EMCCD. He discovered Variable Multiplication Gain Imaging as a method for imaging nearin exo-planets with photon-counting EMCCDs in a High-Contrast Instrument.

Peter Petrone is currently developing and testing optical hardware to validate and refine methodologies for advancing the science of high-contrast nulling interferometry. Prior to this, he was involved in characterizing the HST Advanced Camera for Surveys (ACS) filter set.

Dominic Benford is an astrophysicist with research interests in extragalactic astrophysics and cosmology, with emphasis on the formation and evolution of galaxies and their stars. His primary research background is in instrumentation for far-infrared and submillimeter astronomy.